

## Optical Tamm state on a femtosecond time scale

P. Melentiev, A. Afanasiev, and V. Balykin\*

*Institute for Spectroscopy Russian Academy of Sciences, Phizicheskaya str., 5, Troitsk, Moscow 142190, Russia*

(Received 5 September 2013; published 25 November 2013)

In this work, we investigated the temporal dynamics of the optical Tamm state (OTS) that arises at the interface between a one-dimensional photonic crystal and a gold nanofilm. The temporal dynamics was measured by two methods: (1) the spectral method, which is based on the analysis of the spectral composition of reflected light, and (2) the probe method, i.e., by embedding an inertialess probe into the OTS mode. It was found that the temporal dynamics of OTS formation is determined by the quality factor of the photonic-crystal/nanofilm microcavity with a characteristic time of OTS formation in the range of 100 to 300 fs.

DOI: [10.1103/PhysRevA.88.053841](https://doi.org/10.1103/PhysRevA.88.053841)

PACS number(s): 42.25.Gy, 81.05.Xj, 73.20.Mf, 79.20.Uv

### I. INTRODUCTION

Optical Tamm states (OTSs) [1,2] are the optical analog of electron Tamm states [3]. During recent years, OTSs have become a subject of intense theoretical and experimental research [4–10]. OTSs arise at the surface of a photonic crystal. Media that can border a photonic crystal (PC) are as follows: (i) dielectric media with a positive dielectric constant ( $\epsilon > 0$ ), (ii) dielectric media with a negative dielectric constant ( $\epsilon < 0$ ), (iii) conducting metal, and (iv) another PC [7]. Depending on the physical properties of the medium that borders the PC, a large variety of surface states can occur with a corresponding localization of the electromagnetic field. Physical reasons for the localization of the electromagnetic field are (a) an exponential decay of the field toward the bulk of a medium with a negative dielectric permittivity (an imaginary value of the wave vector in the medium) and (b) a decay of the wave in a medium with a positive dielectric constant that is caused by the implementation of the condition for total internal reflection (in this case the PC plays the role of the medium with a negative dielectric permittivity). From the viewpoint of practical applications, the case of a conducting metal as a PC-adjointing medium seems to be the most interesting. In this case, not only is surface localization of the electromagnetic field possible, but also a considerable enhancement of the field amplitude in the PC/metal-nanofilm system [7,11,12]. In addition, the metal nanofilm on the surface of the PC makes it possible to perform surface nanostructuring in it [11,12]. If the size of the nanostructures is much smaller than the radiation wavelength, the nanostructuring of the film does not destroy the OTS [11,12] which, in turn, opens up an enormous arsenal of nanoplasmonics for controlling light fields via these nanostructures. Therefore, in a PC/metal-nanofilm optical system, it is possible to simultaneously realize (1) plasmonic enhancement of the electromagnetic field and (2) field enhancement with OTSs.

It is well known that the plasmon mechanism of enhancement of the electromagnetic field is based on the low-inertia response of the electron subsystem of the metal. The characteristic time of this mechanism can be shorter than 1 fs [13]. The physical origin of the OTSs is different and is based on constructive interference of electromagnetic waves

in a PC. The objectives of this work are (i) to experimentally study the temporal dynamics of an OTS and (ii) to measure the time of formation of an OTS in an PC/metal-nanofilm optical system.

### II. EXPERIMENTAL SETUP

The schematic of the experimental setup for the temporal dynamics study of the OTS is presented in Fig. 1. It consists of the following basic elements: (i) a femtosecond laser (TiF-50F, Avesta Ltd.), (ii) an optical device for the formation of a laser pulse with the necessary time and spectral characteristics, (iii) the optical sample under study (PC/metal-nanofilm), (iv) an inverted optical microscope (Nikon Eclipse Ti), and (v) a system for the spatial and spectral characterization of the light from the sample under study. The OTS was excited by a femtosecond laser pulse. The radiation was collected by an objective and was directed to a two-dimensional (2D) CCD array for recording the optical image or to a spectrometer for the spectral measurement, and to a photomultiplier tube (PMT) (using a delay line) to obtain a correlation signal and to measure the temporal characteristics of the radiation.

The laser had the following parameters: the radiation wavelength could be tuned from 700 to 900 nm, the pulse duration was  $\tau_{\text{las}} = 66$  fs, the average power was 1 W, and the pulse repetition rate was 80 MHz. The laser can also operate in the continuous regime with the possibility of frequency tuning in the same spectral range. The optical device for the formation of the laser pulse in the spectral and time domains consisted of (a) a laser-beam expander which can increase the beam diameter up to 7 mm and two prisms made of flint glass, (b) two slits, with one of them arranged in front of the prism unit while the other one is placed behind it. An increase in the duration of the laser pulse was achieved due to the increase of the optical depth over the width of the laser beam that was introduced by the prisms. The length of the optical path traveled by the light beam as it propagates through the prisms depends on the position of the point at which the light beam enters the prism; namely, the closer this point is to the prism edge, the smaller is the change in the optical path length of the light beam. Therefore, by changing the cross section of the laser beam with slit (2), which is located behind the beam expander [Fig. 1(b)], we could vary the duration of the pulse from 150 fs to 2 ps. The device also made it possible to vary the spectral composition of the radiation, i.e., its spectral

\*balykin@isan.troitsk.ru; homepage: [www.atomoptics.ru](http://www.atomoptics.ru)

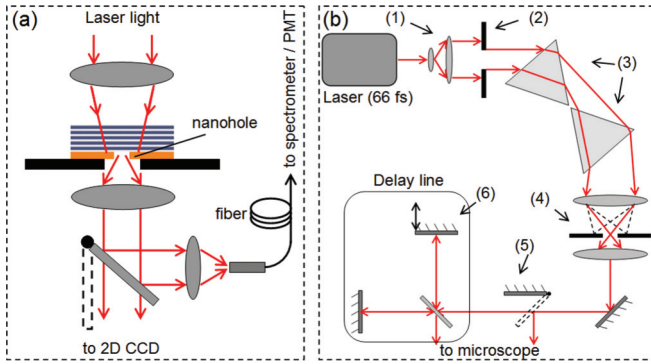


FIG. 1. (Color online) (a) Scheme of measurement of an OTS in a PC/metal-nanofilm system using a Nikon Eclipse Ti inverted microscope. (b) An optical device for the formation of the spectral and temporal characteristics of a laser pulse, which consists of the following elements: (1) a beam expander, (2) a slit with a variable width for controlling the duration of the laser radiation pulse, (3) two prisms made of flint glass, (4) a slit with a variable width for controlling the spectral width of the laser radiation, (5) a flipping mirror, (6) a mirror of the delay line, which is controlled by a stepper motor.

width and central wavelength. For this purpose, a lens was installed behind the prisms in the focal plane of which the second slit was positioned. By choosing the width of this slit and its position, it was possible to form Fourier-transform-limited laser pulses with a pulse duration ranging from 150 fs to 2 ps.

In the experiment the duration of the laser pulse was measured by using the autocorrelator. The correlation function of the first order was measured by using a custom-made delay line (Avesta Ltd.), which was formed by a Michelson interferometer; one mirror of which was moved by a stepper motor. To measure the autocorrelation function of the second order, we used a commercial autocorrelator (AA-20DD, Avesta Ltd.).

The PC of the sample used in this research was fabricated on a quartz substrate in the form of a 12-layer stack of alternating  $\text{TiO}_2$  and  $\text{MgF}_2$  dielectric layers with high and low refractive indices ( $n = 2.23$  and  $1.38$ , respectively) and thicknesses of  $\lambda/4n$  ( $\lambda = 730$  nm; the values of the refractive indices were taken from Ref. [14]). A Au nanofilm with a thickness of 220 nm coated the PC on one side [Fig. 1(a)]. The one-dimensional (1D) PC has a low (about 2%) transmission of light in the spectral range 650–800 nm (the band gap of the PC). The deposition of the gold film made it possible to create an OTS at the PC/metal-nanofilm interface (the resonance wavelength of the OTS is 780 nm [11]). Subsequently, a nanosized object (a nanohole) is created in the gold nanofilm.

To measure the temporal dynamics of the formation of the OTS, we used two experimental methods: (1) a spectral method by which changes in the reflection spectra of the femtosecond laser radiation from the PC/metal-nanofilm were measured and (2) a temporal method that is based on an inertialess instantaneous nanosized probe. In the temporal method, because a nanosized probe was used, a nanohole was made in the gold film of the PC/metal-nanofilm optical system (Fig. 2). Upon irradiation of the PC/metal-nanofilm

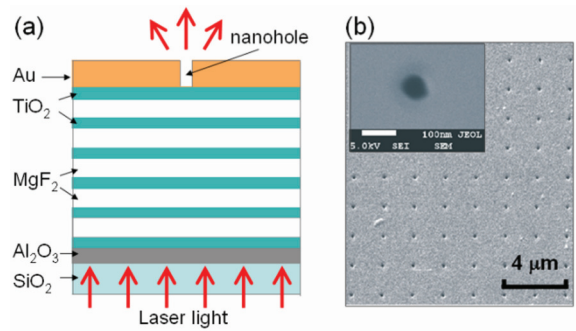


FIG. 2. (Color online) (a) Schematic of a PC/metal-film microcavity formed by 12 dielectric layers and an Au film; (b) an electron-microscope image of a nanohole array made in a Au nanofilm. Nanoholes play the role of an OTS probe. The inset shows an enlarged image of one nanohole.

system, an OTS arises on the inner surface of the metal film [12] and, as a result, the nanohole proves to be embedded in the OTS electromagnetic mode. The OTS considerably enhances the amplitude of the light field incident on the nanohole in the PC/metal-nanofilm [15]. If the diameter of the nanohole is much shorter than the radiation wavelength, the nanostructuring does not deteriorate the OTS [11,15], and the nanohole serves as a nondestructive probe for the OTS.

Measurements with single nanoholes were performed using a Nikon Eclipse Ti inverted microscope. The laser radiation was focused on the PC/metal-nanofilm surface by a  $10\times$  objective with a numerical aperture  $\text{NA} = 0.25$  into a spot with a diameter of about  $4\ \mu\text{m}$ . The radiation scattered by the nanohole was collected by a  $40\times$  objective with a numerical aperture of  $\text{NA} = 0.65$  and recorded with a cooled two-dimensional CCD camera (Photon-MAX, Princeton Instruments, with avalanche electron multiplication). The spectral analysis was performed by using a spectrometer with a cooled CCD array (NTE/CCD-1340/100, Princeton Instruments). A spatial filter was also used at the entrance of the spectrometer to deduce the background signal. To eliminate the influence of mechanical vibrations, the entire setup was installed on a vibration isolation table.

The nanoholes were formed in a gold film of the PC/metal-nanofilm optical structure by using a focused ion beam (FEI Quanta 3D,  $\text{Ga}^+$  ions, 30 keV, 10-nm-diameter spot). The diameter of the nanoholes was 60 nm. The shape and the size of each individual nanohole were measured by electron microscope (JEOL JSM-7001F) with a spatial resolution of about 5 nm. The spacing between nanoholes was  $2\ \mu\text{m}$ . We note that, in this work, measurements were performed with individual nanoholes. Each nanohole had its own marker, which made it possible to unambiguously find this nanohole on the gold film and to detect the optical signal emitted only from this nanohole.

### III. EXCITATION OF OTS WITH PULSED LASER RADIATION

#### A. Spectral measurements of formation of OTS

Experimentally, an OTS can be revealed from measurements of the transmission (or reflection) coefficient of the

PC/metal-nanofilm system as a function of the wavelength of radiation incident on the system. In this case, a narrow peak for the transmittance (or reflectance) is observed at the frequency that corresponds to the OTS. In the stationary case the peak width is determined by the properties of the PC and the metal nanofilm. It should be noted that there is a certain analogy between the PC/metal-nanofilm system and a Fabry-Perot etalon: The PC/metal-nanofilm can be considered as a limiting case of a Fabry-Perot etalon with “zero” spacing between the mirrors. As for the Fabry-Perot etalon, the PC/metal-nanofilm system and, therefore, the OTS can be characterized by the lifetime  $\tau$  of the photon in the OTS mode which, in turn, is determined by the physical parameters of the PC and metal nanofilm. The photon lifetime  $\tau$  is unambiguously related to the resonance width  $\Delta\omega_{\text{OTS}}$  of the transmittance (or reflectance) function of the two optical systems:  $\tau_{\text{OTS}} = \Delta\omega_{\text{OTS}}^{-1}$ . In the experiment, a pulsed laser light was used to excite the OTS. A Fourier-transform-limited laser pulse is characterized by its spectral width  $\Delta\omega_{\text{las}}$ , which is related to the pulse duration  $\tau_{\text{las}}$  by the same relation. It is clear that, at a rather long duration of the laser pulse and, correspondingly, at rather narrow spectral width ( $\tau_{\text{las}} > \tau$ ,  $\Delta\omega_{\text{las}} < \Delta\omega_{\text{OTS}}$ ), a quasistationary regime of the interaction between the laser radiation and the OTS mode is realized, which is characterized by the fact that all photons of the laser pulse are involved in the formation of the OTS mode. In the spectral domain, this means that all spectral components of the laser pulse contribute to pumping of the OTS mode. In the opposite case ( $\tau_{\text{las}} < \tau$ ,  $\Delta\omega_{\text{las}} > \Delta\omega_{\text{OTS}}$ ), a nonstationary regime is realized in which not all photons and not all spectral components of the laser pulse are involved in the pumping of the OTS mode, and part of them are “rejected” by the OTS mode.

Figure 3 shows the results of numerical calculations of the temporal dynamics of the OTS that were obtained by the finite-difference time-domain (FDTD) method (with a calculation accuracy of  $10^{-6}$ ). The OTS was excited by monochromatic

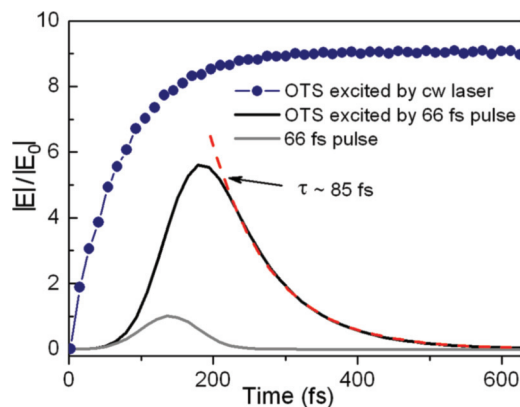


FIG. 3. (Color online) Results of numerical calculations of the temporal dynamics of the electromagnetic-field envelope in the OTS mode: (a) the field envelope when the continuous laser radiation with a wavelength that corresponds to the exact resonance of the OTS is switched on at the moment  $\tau = 0$  (dash-dotted curve), (b) the field envelope in the OTS mode that is excited by a 66 fs pulse (black curve). The envelope of the incident laser pulse is shown by the gray curve.

radiation that was incident on the PC/metal-nanofilm from the side of the dielectric layers of the PC perpendicularly to their surface. The radiation wavelength was equal to the exact OTS resonance value:  $\lambda_{\text{OTS}} \approx 780$  nm. The dash-dotted curve shows an increase in the amplitude of the OTS field upon turning on the continuous radiation (with the step function of the incident field). An analysis shows that this dependence is exponential with a characteristic time  $\tau_1 = 75$  fs. At times  $\tau \gg \tau_1$ , the amplitude of the OTS field achieves its stationary value, which exceeds the amplitude of the incident radiation by approximately a factor of nine.

Figure 3 also presents the results of calculations of the amplitude of the OTS field upon irradiation of the PC/metal-nanofilm by radiation with a pulse duration  $\tau_{\text{pulse}} = 66$  fs and a wavelength that corresponds to the OTS resonance. In this case, a nonstationary regime of the OTS formation is realized. The envelope of the arising OTS field is presented in Fig. 3 by the black curve, while the envelope of the excitation radiation is shown by the gray curve. The calculated envelope of the OTS field is nonsymmetric. Its rising edge is determined by the corresponding edge of the excitation laser pulse, which is smaller than the characteristic time  $\tau_1$  of OTS formation. The falling edge is a long exponentially decaying trailing edge with a characteristic time  $\tau_2 = 85$  fs, which is determined by the photon lifetime in the cavity that is formed by the PC and the metal nanofilm. We note that, at a chosen duration of the excitation radiation ( $\tau_{\text{pulse}} < \tau_1$ ), the maximal value of the amplitude of the OTS field is  $5.7E_0$  and does not attain its stationary value. Therefore, the calculations show that the nonstationary dynamics of the OTS field is realized for pulse durations of the incident radiation  $\tau_{\text{pulse}} < \tau_1 + \tau_2 \approx 160$  fs.

We measured the reflection of laser pulses of different durations ( $\tau_{\text{OTS}} < \tau_{\text{las}}$  and  $\tau_{\text{las}} < \tau_{\text{OTS}}$ ) from the PC/metal-nanofilm optical system and at different wavelengths of the laser pulse with respect to the wavelength of the OTS resonance. As will be shown below, these spectral measurements yield information on the temporal dynamics of the OTS in the PC/metal-nanofilm.

Figure 4 shows the result of excitation of the OTS by a femtosecond laser pulse; in this experiment, we measured the spectrum of the laser pulse reflected from the PC/metal-nanofilm. The irradiation was performed from the side of the dielectric layers with the pulse width  $\tau_{\text{las}} = 66$  fs. This case corresponds to the nonstationary interaction regime. It can be seen from this figure that a narrow dip is observed in the spectrum. The width of this dip at half depth is 4 nm. Calculations show that the measured width of this dip corresponds to the excitation of the OTS mode with a spectral width of 9 nm. Therefore, photons with spectral components near the revealed feature contribute to pumping the OTS mode.

A spectral manifestation of the process of temporal formation of the OTS mode is shown in Fig. 5. We measured the reflectance of the PC/metal-nanofilm optical system as a function of wavelength at different pulse widths:  $\tau_{\text{las}} = 66$  to 2000 fs. Figure 5 presents typical results of these measurements. Figure 5(a) corresponds to excitation by continuous radiation, Fig. 5(b) shows the results with pulsed excitation with  $\tau_{\text{las}} = 300$  fs (which corresponds to the minimal pulse width at which the OTS has already been formed), and Fig. 5(c) presents data for a nonstationary regime of excitation of the OTS with

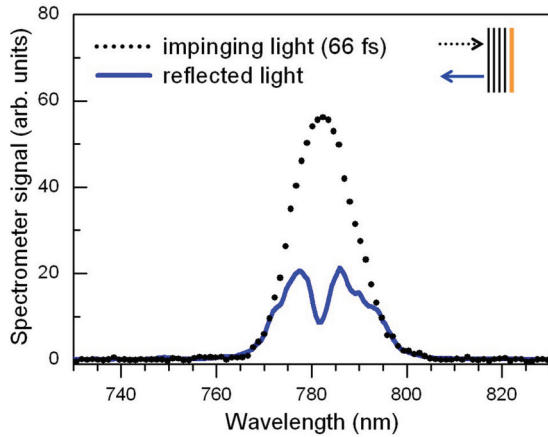


FIG. 4. (Color online) Excitation of an OTS by a femtosecond laser pulse in a PC/metal-film structure. The figure shows the deformation of the spectrum of the femtosecond laser radiation upon its reflection at the boundary the PC/metal-film as a result of the excitation of an OTS (solid curve). The spectrum of the incident radiation is shown by black dots.

a pulse width of  $\tau_{\text{las}} = 66$  fs. To the different pulse widths corresponds the different values of the spectral width. The interaction of the laser pulse with a duration of  $\tau_{\text{las}} = 300$  fs with the PC/metal-nanofilm corresponds to the quasistationary interaction regime, and the measured reflectance curve has the shape of the OTS mode with a width  $\Delta\omega_{\text{ref}} = 13$  nm [Fig. 5(b)]. However, the pulse width  $\tau_{\text{las}} = 66$  fs corresponds already to the nonstationary interaction regime, which leads to a broader profile of the reflectance curve with the width  $\Delta\omega_3 = 20$  nm [Fig. 5(c)]. The observed considerable broadening of the reflectance curve indicates that not all spectral

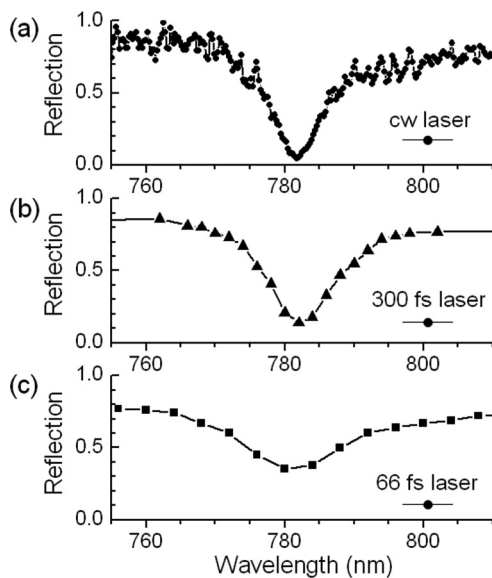


FIG. 5. Spectral manifestation of the process of formation of the OTS mode. Shown is the reflectance of the laser pulse from the PC/metal-nanofilm measured as a function of the laser radiation wavelength at different durations of the laser pulse (a) in the continuous-excitation regime and [(b) and (c)] in the pulsed-excitation regime with  $\tau_{\text{las}} = 300$  and  $\tau_{\text{las}} = 66$  fs.

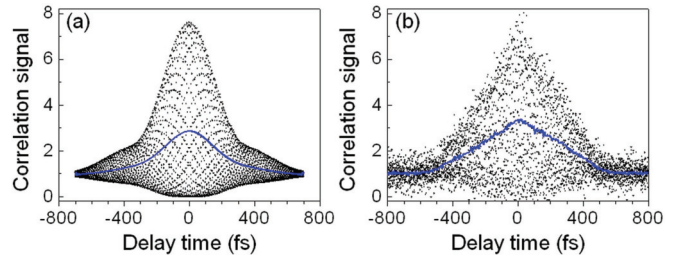


FIG. 6. (Color online) Second-order correlation functions for a Gaussian light pulse reflected from a PC/metal-nanofilm that were (a) calculated (by the FDTD method) and (b) measured for a light pulse width of 300 fs and a wavelength corresponding to the OTS excitation.

components of the laser pulse are involved in the formation of the OTS mode; namely, spectral components that do not correspond to the OTS mode are reflected from the PC. From Fig. 5 we can see a significant difference between the reflectances of the PC/metal-nanofilm system at different pulse durations and at exact OTS resonance: (a)  $r_1 = 6\%$ , (b)  $r_2 = 16\%$ , and (c)  $r_3 = 35\%$ .

The curves of Fig. 5 permit us to evaluate the lifetime of photons in the OTS mode. From the relation  $\tau_{\text{OTS}} = \Delta\omega_1^{-1}$  and Fig. 5(a), the lifetime of photons in the OTS mode can be determined to be  $\tau_{\text{OTS}} > 100$  fs. This lifetime is determined by the quality factor of the PC/metal-nanofilm system.

### B. Temporal measurements of OTS formation

The direct measurement of OTS formation in the PC/metal-nanofilm is a temporal measurement of the reflection from the PC/metal-nanofilm of a laser pulse. To this end, we performed measurements of the second-order autocorrelation function of a light pulse that arises upon reflection of a laser pulse from the PC/metal-nanofilm. At first, we measured the second-order autocorrelation function of the laser pulse itself, and then we measured the second-order autocorrelation function of the light pulse that was reflected from the PC/metal-nanofilm.

Figure 6(b) presents results of measurements of laser radiation with a pulse duration  $\tau_{\text{las}} = 300$  fs upon its reflection from the PC/metal-nanofilm system. The results of the calculations are given in Fig. 6(a). Curves presented in Fig. 6 show that, upon reflection from the PC/metal-nanofilm system, the pulse duration remains the same, which confirms the realization of the quasistationary regime of the OTS excitation.

Figure 7 presents results of measurements that were performed using a laser pulse with a duration of  $\tau_{\text{las}} = 66$  fs. This case corresponds to the nonstationary excitation regime of the OTS mode. Here we investigated the excitation of the OTS mode for different wavelengths of the laser radiation incident on the PC/metal-nanofilm. Figures 7(a), 7(c), and 7(e) present results of measurements of the second-order correlation function for light pulses reflected from the PC/metal-nanofilm at the following laser radiation wavelengths: 750 nm [Fig. 7(a)], 781 nm [Fig. 7(c)], and 810 nm [Fig. 7(e)]. Figures 7(b), 7(d), and 7(f) show the calculated shapes of the envelopes of light pulses reflected from the PC/metal-nanofilm that correspond to the measured second-order correlation functions [Figs. 7(a), 7(c), and 7(e)]. It can be seen from this

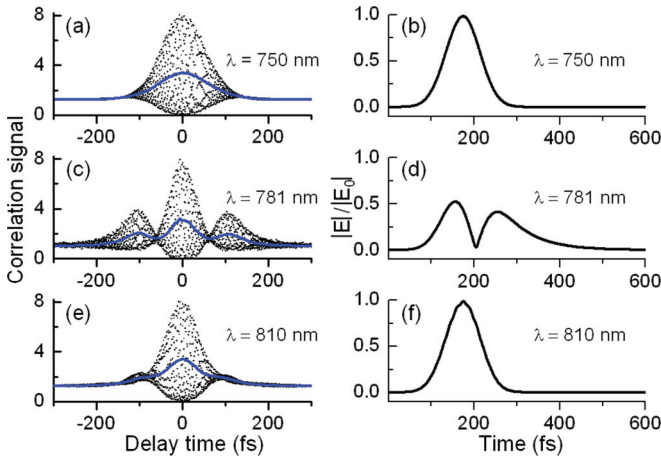


FIG. 7. (Color online) Excitation of the OTS in the PC/metal-nanofilm at different wavelengths of incident laser radiation. Panels (a), (c), and (e) show the measured second-order correlation functions of light pulses reflected from the PC/metal-nanofilm at different wavelengths of laser radiation incident on the PC/metal-nanofilm: (a) 750 nm, (c) 781 nm, and (e) 810 nm. Panels (b), (d), and (f) show calculated shapes of the envelopes of light pulses reflected from the PC/metal-nanofilm that correspond to the measured second-order correlation functions [see panels (a), (c), and (e)].

figure that the shape of the correlation function dramatically depends on the laser radiation wavelength with respect to the resonant length of the PC/metal-nanofilm. When the laser radiation is detuned from the OTS resonance, the shape of the reflected pulse corresponds to that of the incident pulse [Figs. 7(a), 7(b), 7(e), and 7(f)]. In the resonance case, the shape of the correlation function has a complex three-peak structure [Fig. 7(c)], which is characteristic for the case of a double-peak light pulse [Fig. 7(d)]. We note a long exponentially decaying trailing edge of the second pulse [Fig. 7(d)], characterizing the time scale of the OTS decay dynamics (see Fig. 3, black curve). The physical reason that the incident one-component laser pulse is split into a two-component one is that the spectral width of the incident laser pulse is large compared with the spectral width of the OTS participate in the pumping of the OTS mode. The OTS mode is pumped during the characteristic photon lifetime in the OTS mode. Precisely these components of the spectrum of the laser pulse form the trailing part of the reflected light pulse. Components of the spectrum of the laser pulse that are outside of the spectral width of the OTS are reflected from the PC/metal-nanofilm; they do not experience a time delay and are responsible for the unshifted part (with respect to the incident pulse) of the reflected pulse.

#### IV. NANOHOLE AS INSTANTANEOUS OTS PROBE

As was already noted above, there is a certain analogy between the PC/metal-nanofilm system and a Fabry-Perot cavity. The PC/metal-nanofilm can also be considered as a limiting case of a Fabry-Perot microcavity with zero spacing between mirrors. The electromagnetic field inside the Fabry-Perot cavity can be judged from the transmittance (reflectance)

function of the cavity, as well as from the absorption or scattering of light from a quantum-mechanical object placed inside the cavity mode and which plays the role of a probe of the mode field. In this case, the dynamics of the cavity mode can be investigated from the absorption or scattering characteristics of the quantum-mechanical object [16]. A natural requirement imposed on the parameters of the quantum-mechanical object is its high-speed response to the radiation: a characteristic response time should be shorter than the formation time of the cavity mode.

If the optical system is a PC/metal-nanofilm, it is impossible to place any physical object inside the OTS mode due to its zero thickness. We solved this problem in the following way: In the metal nanofilm (which is an intrinsic part of the PC/metal-nanofilm system), a nanohole was created. If the size of this nanohole is considerably smaller than the radiation wavelength, the influence of the nanohole on the characteristics of the OTS mode can be neglected [15]. At the same time, the radiation transmitted through the nanohole is proportional to the instantaneous intensity of the OTS mode. The nanohole can be considered as an inertialess probe object inside the OTS mode.

Figure 8 presents results of measurements of the transmittance of a nanohole in the PC/metal-nanofilm system at different durations of the excitation laser radiation: (a) continuous radiation, (b) pulsed radiation with a pulse width of  $\tau_{\text{las}} = 300$  fs and (c) pulsed radiation with a pulse width of  $\tau_{\text{las}} = 90$  fs. The obtained transmittance curves correspond to different regimes of the OTS excitation. It can be seen from the figure that the case  $\tau_{\text{las}} = 300$  fs almost coincides with the

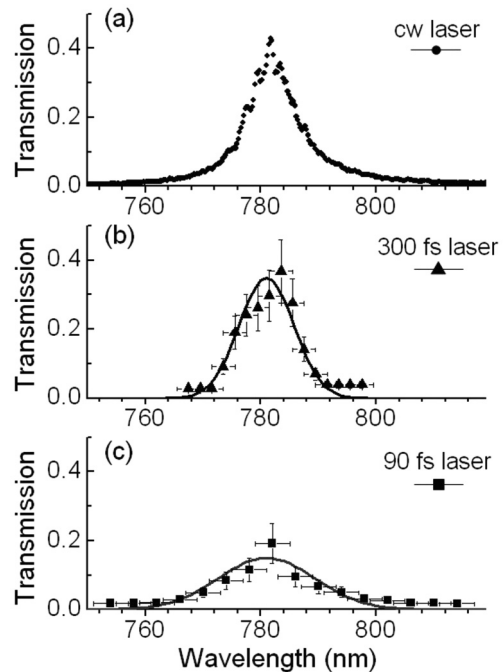


FIG. 8. Measured transmission of a single nanohole with a diameter of 60 nm prepared in a Au layer of a PC/metal-nanofilm as a function of the incident laser radiation wavelength and different regime of excitation: (a) continuous excitation, (b) pulsed excitation with a pulse width of 300 fs, and (c) pulsed excitation with a pulse width of 90 fs.

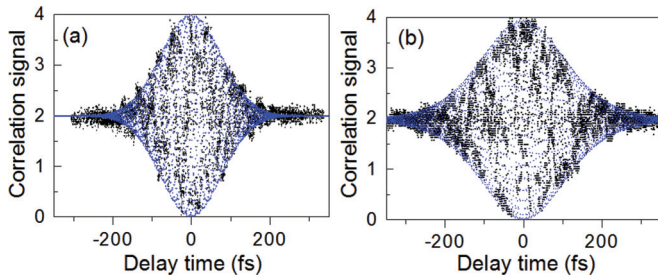


FIG. 9. (Color online) Measured (dotted curves) and calculated (solid curves) first-order correlation functions of the pulsed radiation (90 fs) transmitted through (a) a nanohole with a diameter of 60 nm made in a gold film with a thickness of 200 nm that was deposited on a quartz surface, and (b) a nanohole with a diameter of 60 nm made in a gold film with a thickness of 200 nm that belongs to the PC/metal-nanofilm system.

stationary case: the time duration of 300 fs is quite sufficient for the OTS mode to be formed. At the pulse width of  $\tau_{\text{las}} = 90$  fs, the shape of the curve is different: the intensity at the maximum of the transmittance curve is lower than in the stationary case, which in turn indicates that, within the pulse width of 90 fs, the OTS mode had no time to be formed. At these short pulses, the nonstationary character of the OTS mode also manifests itself in broad wings of the transmittance curves.

Figure 9 presents results of measurements of the first-order correlation functions of the transmitted through a nanohole laser pulse of 90 fs duration. Figure 9(a) corresponds to the use of the nanohole in the gold film (without the PC). Figure 9(b) corresponds to the use of the nanohole in the gold film of the PC/metal-nanofilm system. The correlation function was measured as follows: First, the radiation incident on the specimen was preliminarily transmitted through a delay line [Fig. 1(b)] that was installed immediately behind the laser radiation source. Second, the signal transmitted through the nanohole was detected by a PMT at different delay times.

As can be seen from Fig. 9(a), in the specimen with no PC, the measured correlation function of the first order (black curve) corresponds to the calculated autocorrelation

function for the pulse with a duration of 90 fs (blue curve) and corresponds to the duration of the pulse incident on the nanohole measured with the autocorrelator. The correlation function of the light pulse from the nanohole in the PC/metal-nanofilm system is presented in Fig. 9(b). It is seen that the measured function corresponds to the pulse with a duration of 140 fs. Since the radiation that passed through the nanohole is proportional to the instantaneous intensity of the OTS mode, the measured increase in the duration of the pulse passed through the nanohole is a direct consequence of the inertiality of the OTS mode.

## V. CONCLUSION

Summarizing the performed measurements, we can state that the dynamics of OTS formation is determined by the quality factor of the PC/metal-nanofilm structure. The photon lifetime in the OTS mode that was found from spectral measurements was about 100 fs. Our spectral and autocorrelation measurements with femtosecond radiation show that the amplitude of the OTS field achieves its stationary value at a pulse width of 300 fs. Therefore, the formation time of the OTS lies between 100 and 300 fs. The found values of the temporal characteristics of the OTS were confirmed by the probe method by embedding the inertialess nanosized probe into the OTS mode. We note the importance of our results for applications in nonlinear nanoplasmonics [17] and for the creation of nanolocalized femtosecond sources of laser radiation [18].

## ACKNOWLEDGMENTS

This work was partially supported by the Russian Foundation for Basic Research (projects 11-02-00804, 12-02-00784, 12-02-33073, 13-02-01281), by the Program “Extreme Light Fields” of the Presidium of the Russian Academy of Sciences, and by the Ministry of Education and Science of the Russian Federation. The equipment of the CKP ISAN was used in this work.

- [1] P. Yeh, A. Yariv, and A. Y. Cho, *Appl. Phys. Lett.* **32**, 104 (1978).
- [2] A. P. Vinogradov, A. V. Dorofeenko, S. G. Erokhin, M. Inoue, A. A. Lisyansky, A. M. Merzlikin, and A. B. Granovsky, *Phys. Rev. B* **74**, 045128 (2006).
- [3] I. E. Tamm, *Phys. Z. Sowjetunion* **1**, 733 (1932).
- [4] T. Goto, A. V. Baryshev, M. Inoue, A. V. Dorofeenko, A. M. Merzlikin, A. P. Vinogradov, A. A. Lisyansky, and A. B. Granovsky, *Phys. Rev. B* **79**, 125103 (2009).
- [5] V. N. Konopsky and E. V. Alieva, *Phys. Rev. Lett.* **97**, 253904 (2006).
- [6] T. Goto, A. V. Dorofeenko, A. M. Merzlikin, A. V. Baryshev, A. P. Vinogradov, M. Inoue, A. A. Lisyansky, and A. B. Granovsky, *Phys. Rev. Lett.* **101**, 113902 (2008).
- [7] A. P. Vinogradov, A. V. Dorofeenko, A. M. Merzlikin, and A. A. Lisyanskii, *Usp. Fiz. Nauk* **180**, 249 (2010).
- [8] I. V. Iorsh, P. A. Belov, A. A. Zharov, I. V. Shadrivov, and Y. S. Kivshar, *Phys. Rev. A* **86**, 023819 (2012).
- [9] M. E. Sasin *et al.*, *Appl. Phys. Lett.* **92**, 251112 (2008).
- [10] C. Symonds *et al.*, *Nano Lett.* **13**, 3179 (2013).
- [11] P. N. Melentiev *et al.*, *Opt. Express* **19**, 22743 (2011).
- [12] P. N. Melentiev *et al.*, *JETP* **115**, 185 (2012).
- [13] M. I. Stockman, M. F. Kling, U. Kleineberg, and F. Krausz, *Nat. Photon.* **1**, 539 (2007).
- [14] *Handbook of Optics Technologist*, edited by C. M. Kuznetzova and M. A. Okatova (Mashinostroenie Leningradskoe otdelenie, Leningrad, 1983).
- [15] I. V. Treshin, V. V. Klimov, P. N. Melentiev, and V. I. Balykin, *Phys. Rev. A* **88**, 023832 (2013).
- [16] M. Mücke *et al.*, *Nature (London)* **465**, 755 (2010).
- [17] M. Kauranen and A. V. Zayats, *Nat. Photon.* **6**, 737 (2012).
- [18] T. V. Konstantinova *et al.*, *Quantum Electron.* **43**, 379 (2013).